MCB
Journals.ASM.org

The Extracellular Signal-Regulated Kinase 3 (Mitogen-Activated Protein Kinase 6 [MAPK6])–MAPK-Activated Protein Kinase 5 Signaling Complex Regulates Septin Function and Dendrite Morphology

Frank Brand,[a] Stefanie Schumacher,[a] Shashi Kant,[a,b] Manoj B. Menon,[a] Ruth Simon,[c] Benjamin Turgeon,[d,e] Stefan Britsch,[c] Sylvain Meloche,[d,e,f] Matthias Gaestel,[a] and Alexey Kotlyarov[a]

Institute of Physiological Chemistry, Hannover Medical School, Hannover, Germany[a]; Program in Molecular Medicine, University of Massachusetts Medical School, Worcester, Massachusetts, USA[b]; Institute of Molecular and Cellular Anatomy, Ulm University, Ulm, Germany[c]; and Institut de Recherche en Immunologie et Cancérologie[d] and Departments of Pharmacology[e] and Molecular Biology,[f] Université de Montréal, Montreal, Quebec, Canada

Mitogen-activated protein kinase-activated protein (MAPKAP) kinase 5 (MK5) deficiency is associated with reduced extracellular signal-regulated kinase 3 (ERK3) (mitogen-activated protein kinase 6) levels, hence we utilized the MK5 knockout mouse model to analyze the physiological functions of the ERK3/MK5 signaling module. MK5-deficient mice displayed impaired dendritic spine formation in mouse hippocampal neurons *in vivo*. We performed large-scale interaction screens to understand the neuronal functions of the ERK3/MK5 pathway and identified septin7 (Sept7) as a novel interacting partner of ERK3. ERK3/MK5/Sept7 form a ternary complex, which can phosphorylate the Sept7 regulators Binders of Rho GTPases (Borgs). In addition, the brain-specific nucleotide exchange factor kalirin-7 (Kal7) was identified as an MK5 interaction partner and substrate protein. In transfected primary neurons, Sept7-dependent dendrite development and spine formation are stimulated by the ERK3/MK5 module. Thus, the regulation of neuronal morphogenesis is proposed as the first physiological function of the ERK3/MK5 signaling module.

Extracellular signal-regulated kinase 3 (ERK3) (mitogen-activated protein kinase 6 [MAPK6]) and ERK4 (MAPK4) belong to the group of atypical MAPKs which display a SEG motif in the activation loop (instead of TEY) and carry a long C-terminal extension (1, 15, 58). The regulation, substrate specificity, and physiological functions of atypical MAP kinases are not completely understood (7). The phosphorylation of ERK3 and ERK4 at the serine residue in their activation loop proceeds through upstream protein kinase(s), such as the recently identified p21-activated protein kinases (PAKs) (8, 10), and leads to their activation (6, 9, 37). ERK3 also interacts with the protein phosphatase Cdc14A and is probably an *in vivo* substrate for this enzyme (16). The recent targeted deletion of ERK3 in mouse indicates that this enzyme is essential for neonatal survival and critical for the establishment of fetal growth potential and pulmonary function. The surviving ERK3-deficient pups show reduced reflexes and diminished ability to suckle (25). In contrast, the targeted inactivation of ERK4 in mice does not compromise the embryonic development, viability, and fertility of these animals and does not exacerbate the ERK3 phenotype, but it leads to a depression-related behavior in a forced swimming test (38).

Only one substrate has been described for ERK3 and ERK4 so far, namely, the MAPK-activated protein (MAPKAP) kinase MK5 (also known as PRAK) (1, 19, 41, 42). MK5 binds to ERK3 and ERK4 via a novel MAPK interaction motif (2). An increased level of cytoplasmic ERK3 causes the nuclear-cytoplasmic translocation of MK5, the formation of ERK3/MK5 signaling complexes, and the subsequent activation of MK5 by phosphorylation. The findings that the small interfering RNA (siRNA)-mediated knockdown of ERK3 reduces intracellular MK5 activity (1) and that the ERK3 level is reduced in MK5-deficient cells (41) clearly demonstrate the functional existence of these signaling complexes *in vivo*. The phenotype of the targeted deletion of MK5 in mice does not exactly resemble that of ERK3, but it similarly leads to incomplete postnatal lethality at postnatal day 1 (P1), which depends in its severity on the genetic background (41, 44). The transgenic overexpression of constitutively active MK5 (caMK5) in mice led to anxiety-related traits and locomotor differences (13).

So far, no downstream targets of the ERK3/MK5 signaling module have been identified. However, MK5/PRAK has also been identified as a component of a signaling complex formed with p38 MAPKα/β (34, 46). The p38α/PRAK module is proposed to directly phosphorylate p53 and to contribute to Ras-induced tumor suppression and senescence (50). The p38β/PRAK module is activated by energy depletion, directly phosphorylates Rheb (Ras homologue enriched in brain), a key component of the mTORC1 pathway, and inhibits mTORC1 activation (57). In addition, a p38- and ERK3-independent activation of MK5 by cyclic AMP (cAMP)-mediated protein kinase A (PKA) stimulation was recently reported (45). Furthermore, MK5/PRAK is involved in regulating the expression of the oncogenic transcription factor c-myc at a key position. While being itself a target of transcriptional activation by c-myc, MK5 phosphorylates the transcription factor FoxO3a, which activates mir-34b/c induction and c-myc suppres-

Received 29 November 2011 **Returned for modification** 25 January 2012
Accepted 5 April 2012
Published ahead of print 16 April 2012
Address correspondence to Matthias Gaestel, gaestel.matthias@mh-hannover.de.
Supplemental material for this article may be found at http://mcb.asm.org/.

doi:10.1128/MCB.06633-11

sion, thus forming a feedback loop of the regulation of the intracellular level of c-myc, which is lost in colorectal tumor proliferation (26).

Septins are an evolutionarily conserved family of cytoskeletal GTP-binding proteins that assemble into filaments *in vitro* and *in vivo* (33). In the yeast *Saccharomyces cerevisiae*, septins are involved in the regulation of cytokinesis, and the control of their phosphorylation state is necessary for proper septum formation and the completion of cytokinesis (11). Recent mechanistic studies of septin organization by polarized fluorescence microscopy in living yeast indicate filament reorganizations which support the hypothesis of a mechanical function of yeast septins in cell division (54).

Mammalian septins appear to form a multifunctional network of heteropolymers involved in different processes, such as the control of cell polarity and secretion, cortical organization, and cell cycle regulation, as well as dendritic spine and cilium formation (3, 4, 20, 22, 23, 31, 49). They often exist in heterooligomeric complexes of defined stoichiometry (21). A simple three-component septin complex of Sept2, Sept6, and Sept7 is structurally conserved between mammals and drosophila (47a). The downregulation of Sept2 in mammalian cells by siRNA has recently been demonstrated to reduce Sept6 and Sept7 as well. Furthermore, the downregulation of these three mammalian septins resulted in a lack of chromosome segregation and incomplete cytokinesis, indicating that septins are also essential mitotic components in mammals (48). The assembly of the septin complexes is often regulated by Cdc42 effector proteins, such as Binder of Rho GTPases (Borgs), which also bind to septin GTPases. The ectopic expression of Borg proteins disrupts septin filaments, and Cdc42 GTPase inhibits this effect by blocking the binding of the Borgs to Sept7 (18).

It has been shown that the overexpression of Sept7 increased dendrite branching, and that upon its downregulation dendrite branching was impaired, indicating the importance of septins in mammalian hippocampal neurons (51, 55). These findings support the notion that Sept7, together with other proteins known to control the morphology of dendritic spines, such as the GDP-exchange factor kalirin-7 (Kal7) (56), contributes to the functional plasticity of neurons.

MK5 deficiency is associated with reduced ERK3 levels, thus the MK5 knockout mouse forms the best experimental model to dissect the functions of the ERK3/MK5 signaling module. Here, we analyzed brain morphogenesis in MK5-deficient mice and detected significantly reduced dendritic spine formation in the hippocampus. To identify novel downstream targets of the ERK3/MK5 signaling complex involved in this neuronal phenotype, we did a large-scale interaction screen using neuronal cDNA expression libraries. Mammalian Sept7 (Cdc10) was identified as a novel ERK3 interacting protein by the use of a Ras recruitment system. In a parallel classical yeast two-hybrid (Y2H) screen, Kal7 was identified as an interacting protein and *in vitro* substrate of MK5. Further evidence is provided that Sept7, ERK3, and MK5 exist in the same complex and, together with Kal7, are of physiological relevance in neuronal plasticity by regulating dendritic spine formation.

MATERIALS AND METHODS

Plasmids and antibodies. pECFP, pEGFP, and pEYFP were purchased from Clontech. pEGFP-ERK3, pDEST27 (for the mammalian expression of MK5 and ERK3), and pcDNA6/BioEase (for the mammalian expression of ERK3) were described earlier (41). pEGFP-MK5 was provided by Ole-Morten Seternes (University of Tromso, Norway). pcDNA3-GFP or pcDNA3-Flag and pRK5-myc mammalian expression vectors for mouse Sept7 were provided by Koh-ichi Nagata (Aichi Human Service Center, Japan). pDEST27-Sept7 was purchased from Invitrogen. pGEX-4T3-Kal7/SR3-6 and pGEX-4T3-Kal7/SR4-7 were a gift of Betty Eipper (University of Connecticut). Bacterial expression plasmids for Borg1, Borg2, and Borg3 were a gift from Ian Macara (University of Virginia School of Medicine).

Anti-green fluorescent protein (anti-GFP) (B-2), anti-glutathione *S*-transferase (anti-GST) (B-14), antihemagglutinin (anti-HA) (Y-11), and anti-myc (9E10) antibodies were purchased from Santa Cruz Biotechnology. Antibodies against ERK3 were from Cell Signaling Technology, antibodies against MK5 were from Sigma-Aldrich, and antibodies against Sept7 were purchased from IBL Japan.

Cloning and site-directed mutagenesis. For the cloning of ERK3CT into pENTR/D-TOPO (Invitrogen), the open reading frame of mouse *Erk3* cDNA was amplified from the cDNA clones by PCR using the primer pair 5′-CAC CAG CAT CTA CTC CTT CCC GA-3′ (forward) and 5′-TTA GTT CAG ATG TTT CAG AAT GCT GC-3′ (reverse). The recombination reactions between the entry clone and the pDEST27 and pcDNA6/BioEase-DEST vectors for GST- and BioEase (BE)-tagged ERK3 expression in mammalian systems were achieved with the LR clonase kit (Invitrogen). C-terminal deletion mutants of ERK3, ERK3ΔC1, ERK3ΔC2, and ERK3ΔC3 were generated as described elsewhere (19).

For the cloning of Sept7 and its different deletion mutants into pENTR/D-TOPO (Invitrogen), the open reading frame of mouse Sept7 cDNA was amplified from the pCMV-SPORT6-SEPT7(IRAVp968C04100D6-RZPD) plasmid by PCR using the following primer pairs: for Sept7, 5′-CAC CAT GTC GGT CAG TGC GAG ATC-3′ (forward) and 5′-TTA AAAGAT CTT GCC TTT CT-3′ (reverse); Sept7ΔC, 5′-CAC CAT GTC GGT CAG TGC GAG ATC-3′ (forward) and 5′-CTT GTT GTT ATC CAC TCC AT-3′ (reverse); Sept7ΔN, 5′-CAC CTT ATA CTT CAT TGC TCC TTC-3′ (forward) and 5′-TTA AAAGAT CTT GCC TTT CT-3′ (reverse); and Sept7ΔCΔN, 5′-CAC CTT ATA CTT CAT TGC TCC TTC-3′ (forward) and 5′-CTT GTT GTT ATC CAC TCC AT-3′ (reverse). The recombination reactions between the entry clone and the pDEST27 and pcDNA6/BioEase-DEST vectors were performed as described above.

The cloning of ECFP-Sept7 and EYFP-ERK3 was performed by restriction-free cloning (53). Sept7 was amplified from pSport6-Sept7 using the primer set 5′-CGA GCT CAA GCT TCG AAT TCG ATG TCG GTC AGT GCG AGA TCC-3′ (forward) and 5′-TAC CGT CGA CTG CAG AAT TCT TAA AAG ATC TTG CCT TTC TTC TTG TTC-3′ (reverse). ERK3 was amplified from pDEST27-ERK3 using the primer set 5′-CGA GCT CAA GCT TCG AAT TCG ATG GCA GAG AAA TTC GAA-3′ (forward) and 5′-TAC CGT CGA CTG CAG AAT TCT TAG TTC AGA TGT TTC AG-3′ (reverse). Amplicons were inserted into the target vector pECFP-C1 and vector pEYFP-C1 by PCR.

The Kal SR3-6 S487A mutation was generated using the following primer set: 5′-GTC CTG CAG CGT CCC CTG GCC CCT GGG AAC-3′ (forward) and 5′-ATC CAG CAG TGC TTT CCC ATC CTG GCT GA C-3′ (reverse). Site-directed mutagenesis was performed according to the Phusion standard protocol (Thermo Scientific). As the template, pGEX4T3-Kal7/SR3-6 was used in PCR.

Cell culture and transfection. HEK293 cells were cultured in Dulbecco's modified Eagle medium (DMEM) (Invitrogen) containing 10% fetal calf serum, 2 mM L-glutamine, 100 U of penicillin G/ml, and 100 μg streptomycin/ml (all purchased from PAA). For transfection, cells were seeded 24 h earlier to reach approximately 90% confluence. Transfection was performed using polyethylenimine (PEI; Sigma-Aldrich) at a ratio of 2:1 to the plasmid DNA used, and complex formation was done in Opti-MEM (Invitrogen). Transfected cells were analyzed between 24 and 48 h posttransfection. The transfection of primary hippocampal neurons was

performed according to the standard protocol for the Effectene reagent (Qiagen).

GST pulldown from lysate of transfected HEK293 cells. A total of 5×10^6 transfected HEK293 cells expressing GST-tagged forms of ERK3, ERK4, or Sept7 and their different deletion mutants together with BioEase-tagged forms of wild-type (WT) ERK3, ERK4, and Sept7ΔN were washed with ice-cold phosphate-buffered saline (PBS) and lysed in 1 ml of lysis buffer containing 1% (vol/vol) Triton X-100, 10% (vol/vol) glycerin, 150 mM NaCl, 50 mM HEPES, pH 7.5, 1.5 mM $MgCl_2$, and 1 mM EGTA for 30 min on ice. After centrifugation (16,000 × *g*, 4°C), the supernatant was transferred to a new tube and incubated with 25 μl of glutathione-Sepharose 4B beads (GE Healthcare) with overnight tumbling at 4°C. Protein interactions were analyzed by Western blotting using horseradish peroxidase (HRP)-conjugated streptavidin (Invitrogen) as described previously (41).

***In vitro* kinase assays.** GST-tagged Borg1 to Borg3 proteins and His-tagged Sept7ΔC or Sept7ΔN were expressed in *Escherichia coli* BL21. Kinase assays were performed after pulldown using 15 μl of a 50% suspension of recombinant protein bond to glutathione-Sepharose (Amersham Biosciences) or nickel-nitrilotriacetic acid (Ni-NTA)-agarose and 2.5 μl of buffer (500 mM sodium β-glycerophosphate, 1 mM EDTA, pH 7.4), and recombinant untagged MK5, GST-tagged p38, or His-tagged ERK3 (Sf9 preparation; kind gift of Ole-Morten Seternes) was added in the desired combinations. For the inhibition of p38 kinase activity, an additional 10 μM SB203580 (Calbiochem) was used. The reaction mixture was filled up to a final volume of 20 μl. As a control, 10 μg of substrate recombinant Hsp25 or myelin basic protein (MBP) (Millipore) was used. Five μl of hot ATP mixture (20 mM $MgCl_2$, 0.5 mM ATP, 0.1 μl of 1-μCi [γ-^{33}P]ATP) was added, and the reaction mix was incubated for 1 h at 30°C. Radioactivity incorporated into substrates was quantified by phosphorimaging using a Fuji FLA9000.

Ras recruitment system (RRS). The yeast screening system for the analysis of protein-protein interaction was developed and provided by Ami Aronheim (The Rappaport Institute, Israel). The method is based on an inactive cytosolic Ras mutant (lacking the carboxy-terminal CAAX box), which is fused to the bait protein and unable to bind to the plasma membrane. The Ras mutant can be activated only if the bait protein interacts with its prey, which is permanently bound to the membrane via myristylation. Stringency for the survival of yeast cells is achieved by using a yeast strain, referred to as CDC25-2, carrying a temperature-dependent active Ras mutant. ERK3 was cloned into p425-Met25-Ras(61)ΔF bait vector and stepwise transfected into CDC25-2 yeast cells together with a mouse brain cDNA library in the pYes-M expression vector. Yeast clones were amplified in synthetic minimal medium lacking leucine and uracil (SDΔLU medium) but containing glucose for 5 days at 24°C and selected on SDΔLU medium plates (with an additional lack of methionine) with galactose for a further 4 days at 36°C. Selected yeast clones survive at 36°C on SDΔLU medium with galactose only but not with glucose or additional methionine. From positive clones, prey plasmid DNA was isolated and sequenced. For further analysis, resulting cDNA fragments were cloned into pEGFP vector and used for pulldown interaction experiments.

Yeast two-hybrid screen. A pretransformed mouse brain Matchmaker pACT2-cDNA library (MY4008AH; Clontech) in strain Y187 (*MAT*α) was mated with pGBKT7-MK5-transformed AH109 (*MAT***a**) and plated on 20 SDΔAHLT plates (lacking adenine, histidine, leucine, and tryptophan). The plates were incubated for 3 to 21 days at 30°C. About 10^6 clones were screened. Prey plasmids were isolated and used for retransformation experiments to confirm bait-prey interactions.

Immunofluorescence microscopy. Cells were fixed with 4% paraformaldehyde (PFA) in PBS for 15 min at 4°C and permeabilized with 0.25% Triton X-100–PBS for 20 min at room temperature (RT). Blocking was done using 6% bovine serum albumin (BSA) for 1 h at RT. Anti-HA, anti-myc, anti-Flag, and anti-septin7 antibodies were used at a 1:200 dilution in 1% BSA–PBS for 1 h. Secondary antibodies or Alexa Fluor 488-conjugated streptavidin (Invitrogen) was used at a 1:500 dilution in 1% BSA–PBS. Imaging was performed using a Leica TCS SP2 confocal microscope with constant settings.

Fluorescence resonance transfer (FRET) measurements were performed in living HeLa cells by the acceptor photobleaching technique (29) using a Leica TCS SP2 confocal microscope. The fluorescence of the donor ECFP-Sept7 was excited at 458 nm and detected between 465 and 500 nm before and after the bleaching of the acceptor EYFP-ERK3 at 514 nm. FRET efficiency ranged between 0.05 and 0.95 and was false color coded across this range.

Isolation and retroviral transduction of primary ERK3/MK5-deficient MEFs. Primary mouse embryonic fibroblasts (MEFs) of ERK3/MK5 double-deficient mice were isolated from embryonic day 13.5 (E13.5) embryos and immortalized by cotransfection with pSV40Tag encoding simian virus 40 large T-antigen and pREP8 plasmid (Invitrogen). EcoPack 2-293 cells (Clontech) were used for virus production, and retroviral rescue was performed by sequential infection with pMMP-MK5 and pMMP-ERK3 or of the empty retroviral vector. MEFs were seeded on glass coverslips and fixed with 4% PFA. The indirect immunostaining of endogenous Sept7 was performed using polyclonal anti-Sept7 antibody (IBL Japan) and the corresponding Alexa Fluor 488-conjugated secondary antibody.

Isolation of primary hippocampal neurons. Hippocampal neurons were isolated from E18 BALB/c mice and plated on glass coverslips coated with 200 μg/ml poly-L-lysine (Sigma-Aldrich). Neuronal cultures were grown in neurobasal medium (Invitrogen), 2% B27 supplement (Invitrogen), 1% N2 supplement (Invitrogen), 2 mM L-glutamine (PAA), 25 μg/ml 7S NGF (Calbiochem), 100 U of penicillin G/ml, and 100 μg streptomycin/ml.

Transfection of primary neurons and Sholl analysis of dendritic branching. For the determination of dendritic branching after transfections of ERK3, MK5, and Sept7, primary neurons were cultivated on poly-L-lysine-coated coverslips. Transfection was done at 5 days of *in vitro* culture (DIV5) or DIV10 with pcDNA6/BioEase-ERK3, pcDNA3.1-HA-MK5, or pRK5-myc-Sept7 by following the standard protocol for the Effectene reagent (Qiagen). For the visualization of transfected neurons, pEGFP was cotransfected as well. Seventy-two or 120 h posttransfection, neuronal cultures were fixed with 4% PFA for 15 min at 4°C. The imaging of GFP-positive neurons was performed using a Leica TCS SP2 confocal microscope with constant settings. Generated three-dimensional projections were analyzed using the ImageJ (NIH, Bethesda, MD) software with the Sholl analysis plugin (v1.0; University of California, San Diego, CA).

***In vivo* spine morphology.** Brains of adult MK5 knockout and wild-type animals carrying the Thy1-yellow fluorescent protein (YFP) transgene [breeding with B6.Cg-Tg(Thy1-YFPH)2Jrs/J; Jackson Laboratories] were fixed in 4% paraformaldehyde overnight, followed by embedding in 4% low-melting-point agarose in PBS. One hundred- to 150-μm vibratome sections were prepared, and confocal images (Leica Sp5II) were taken for spine number analysis using ImageJ.

Golgi stain of MK5-deficient and wild-type animals was carried out according to the modified protocol of Heimrich and Frotscher (17).

RESULTS

Impaired spine formation in MK5-deficient neurons *in vivo*. We previously showed the strong coexpression of ERK3 and MK5 in embryonic forebrain (19). Both MK5 and ERK3 are also strongly expressed in the adult mouse brain (27, 38). Erk3$^{-/-}$ newborn mice that survive neonatal lethality display uncoordinated movements, lack of reflex, diminished ability to suckle, and other phenotypes often correlated with neuronal dysfunction (25, 52). In addition, transgenic mice expressing a constitutively active mutant of MK5 develop behavioral abnormalities (13). These observations suggested a neuronal function for the ERK3/MK5 signaling module. As an initial step to monitor any evident neuronal abnormality, we compared Golgi-stained hippocampal sections of

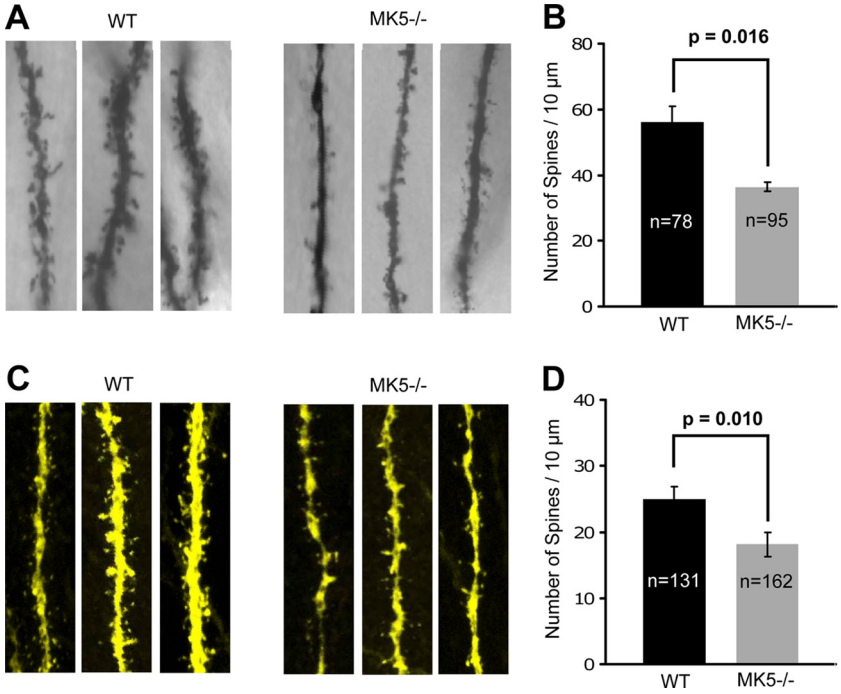

FIG 1 Determination of spine numbers for MK5 deficiency in mice *in vivo*. (A) To visualize hippocampal neurons, Golgi staining was performed with 150-μm vibratome sections of three age-matched WT and MK5$^{-/-}$ mice each. Representative images for each of the animals are shown. (B) Statistical analysis of spine number from three animals of each genotype by one-tailed *t* test. The numbers of dendrites analyzed were 78 (WT) and 95 (MK5 knockout). (C) Analysis of dendritic spines from WT and MK5$^{-/-}$ animals expressing neuron-specific Thy1-YFP reporter protein. Representative images for each of the animals are shown. (D) Statistical analysis of spine number from three animals of each genotype. The numbers of dendrites analyzed were 131 (WT) and 162 (MK5 knockout).

brains of adult MK5-deficient (Mapkapk5tm1Mgl [44]) and WT animals. Golgi staining is a classical histology technique that allows the detailed visualization of neurons in brain sections (17). Interestingly, the analysis of dendritic spine numbers by bright-field microscopy and image analysis reveals a significantly lower number of dendritic spines in this region in the MK5-deficient animals (Fig. 1B). Representative images of WT and MK5 knockout brains are shown in Fig. 1A.

For an independent verification of these results, we crossed the MK5-deficient mice with Thy1-YFP transgenic mice that express YFP at high levels in motor and sensory neurons, as well as subsets of central neurons (12). In these mice, pyramidal neurons are selectively labeled in the hippocampus, hence this line provides a strong and specific Golgi-like vital marker for this neuronal subset with minimal labeling of nearby axons. Typical YFP-stained dendrites of these mice (MK5) and those of wild-type mice carrying only the YFP transgene (WT) are shown in Fig. 1C. Image analysis demonstrates the significant difference between the genotypes (Fig. 1D). These results are in line with the Golgi stain and confirm a role of MK5 in spine formation *in vivo*.

Identification of novel ERK3 interacting proteins by the RRS. The dissection of the novel neuronal functions demanded the identification of ERK3/MK5 interaction partners. Since ERK3 showed intrinsic transactivating properties and, hence, was not suited to be bait in the classical yeast two-hybrid system, we used the RRS for screening a mouse brain cDNA library (5). Potential prey clones (2×10^5) were screened, and eight of the clones isolated showed growth at 36°C under galactose-inducing conditions. Plasmids were rescued, and cDNA inserts representing Cdc25, ubiquitin-like protein 3, and Sept7 were identified. Membrane-bound nucleotide exchange factor Cdc25 could activate the yeast Ras independently of the bait protein and was regarded as a possible false-positive candidate. Nevertheless, the cDNA inserts of Cdc25, ubiquitin-like protein 3, and Sept7 were recloned into mammalian expression vectors and analyzed for ERK3 interaction by pulldown assays. Only Sept7 specifically interacted and coprecipitated with ERK3 on par with MK5 (see Fig. S1 in the supplemental material).

Verification and characterization of Sept7-ERK3 interaction. A possible neuronal ERK3/MK5-Sept7 signaling module is interesting, since a critical role for Sept7 in spine morphogenesis and dendrite development has already been established (51). Therefore, we further analyzed ERK3-Sept7 interaction in more detail. To characterize the regions in Sept7 and ERK3 which are responsible for the interaction, we used appropriate deletion mutants of both proteins (Fig. 2A and FB). The C-terminal part of Sept7 carrying the variable coiled-coil (CC) domain is necessary for the binding of ERK3, since its deletion (Sept7ΔC) completely abolishes interaction with BioEase (BE)-tagged ERK3 (Fig. 2C). The C-terminal extension of ERK3 is responsible for Sept7 interaction, since sequential deletions of the C-terminal extensions of ERK3 reduce (ERK3ΔC1 mutants) or almost completely abolish (ERK3ΔC2 and ERK3ΔC3 mutants) interaction with BE-tagged Sept7ΔN (full-length BE-tagged Sept7 is poorly expressed in HEK293 cells) (Fig. 2D). The binding region for MK5 in ERK3 has been localized to the FRIEDE motif between amino acids 332 and 342 (2), and the ERK3ΔC2 mutants of ERK3 (and ERK4) are still able to bind to MK5 (19, 41). Hence, Sept7 obviously binds to a

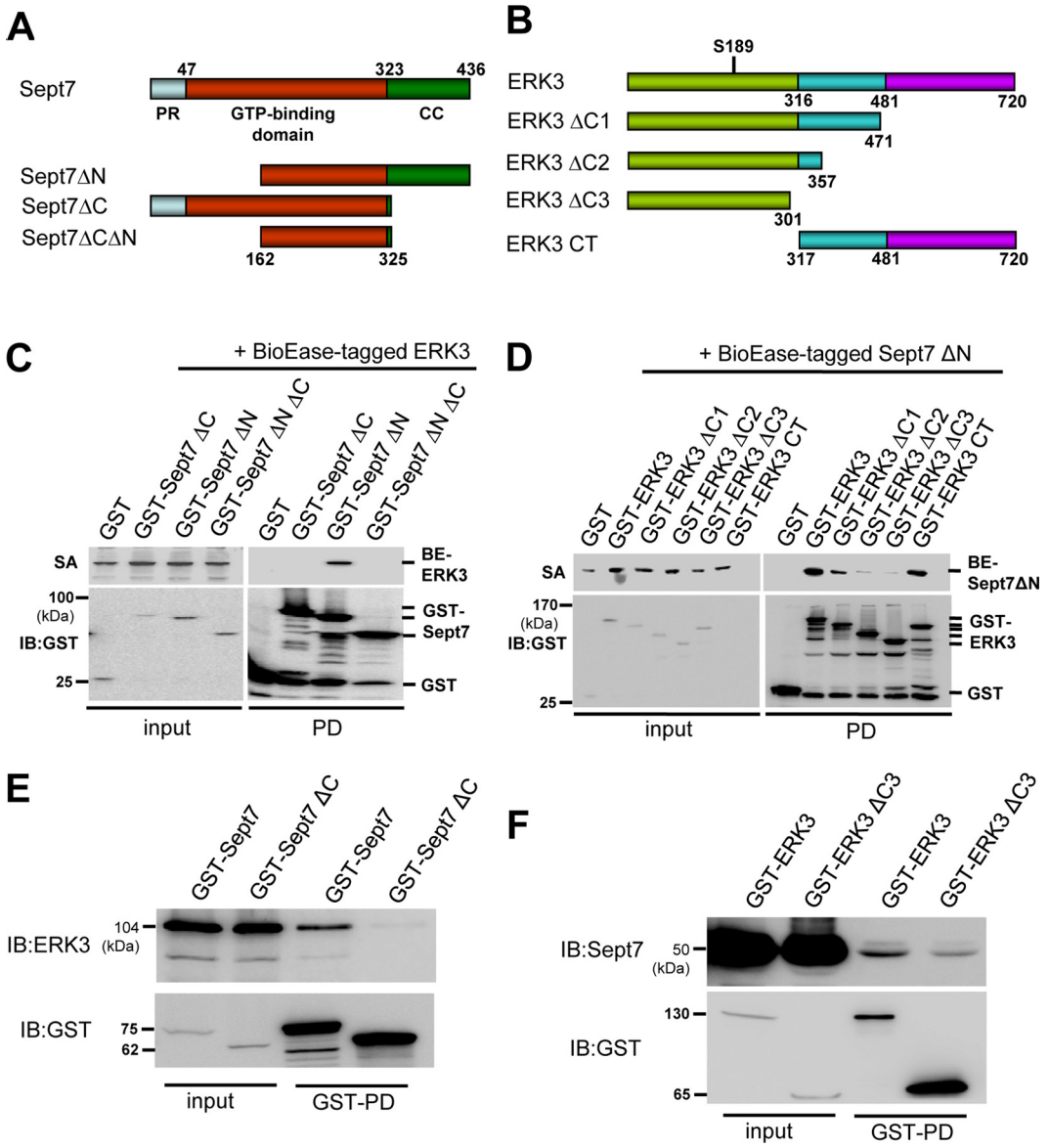

FIG 2 Characterization of the ERK3-Sept7 interaction. (A) Schematic representation of deletion constructs of Sept7 generated for pulldown studies (PR, proline rich; CC, coiled-coil domain). (B) Scheme representing the ERK3 deletion mutants. The activating phosphorylation site is indicated. (C) GST-tagged deletion mutants of Sept7, which lack either or both the C and N termini, were used in a GST pulldown (PD) of BE-tagged ERK3. Only Sept7 with the complete C terminus (CT) can bind to ERK3. IB, immunoblot. SA, streptavidin detection of Bio-Ease tag. (D) Pulldown of BE-tagged Sept7ΔN with GST-tagged C-terminal deletion mutants of ERK3. The region of ERK3 between amino acids 358 and 720 (ΔC2) is essential for effective interaction with Sept7ΔN. (E) Pulldown of endogenous ERK3 by overexpressed GST-Sept7, but not by GST-Sept7ΔC, from lysates of HEK293 cells. (F) Pulldown of endogenous Sept7 by GST-ERK3 from lysates of HEK293 cells. The level of Sept7 in the pulldown is reduced when GST-ERK3ΔC3 is used.

more C-terminal part of ERK3 (ERK3ΔC2; amino acids 358 to 720), and the interaction of MK5 and Sept7 with neighboring but distinct regions in the C terminus of ERK3 might occur.

To further establish the cellular relevance of this interaction and to exclude nonspecific effects of ectopic coexpression, we also attempted to detect the interaction of the endogenous proteins by pulldown with the tagged partner protein. GST-Sept7, but not GST-Sept7-ΔC, is able to pull down endogenous ERK3 from lysates of HEK293 cells (Fig. 2E). Similarly, GST-ERK3 is able to bind endogenous Sept7 from lysates of HEK293 cells (Fig. 2F). These results confirm the presence of a specific interaction between both proteins.

Sept7, ERK3, and MK5 colocalize and form a ternary complex in transfected cells. To prove the relevance of the septin7-ERK3 interaction, we further analyzed the subcellular localization of both proteins. In HEK293 cells, myc-tagged Sept7 shows a heterogeneous filamentary subcellular distribution (Fig. 3A), which partially colocalizes with endogenous actin structures (not shown). BE-tagged ERK3 is diffusely distributed in the cytoplasm and nucleus (Fig. 3A). Interestingly, when myc-Sept7 and BE-ERK3 are coexpressed, both proteins colocalize in distinct filamentous cytoplasmic structures (Fig. 3A). Consistently with this, the coexpression of Flag-tagged Sept7 in HeLa cells changed the uniform cytoplasmic localization of GFP-ERK3 to a more filamentous pattern (Fig. 3B). To demonstrate

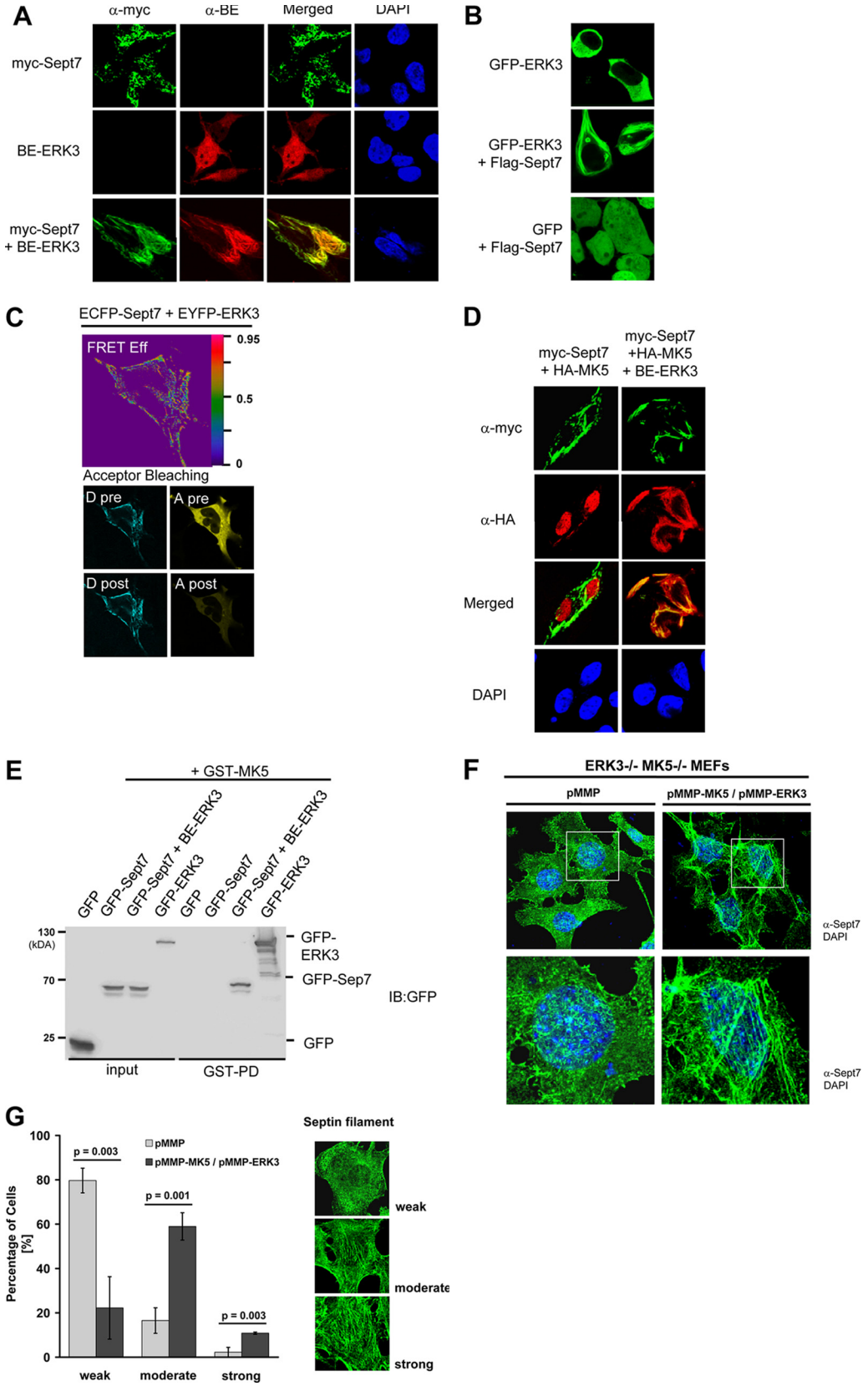

FIG 3 ERK3 acts as a docking platform for Sept7 and MK5. (A) Coexpression of BE-tagged ERK3 with myc-tagged Sept7 leads to the subcellular relocalization of ERK3 to Sept7 filament in HEK293 cells. (B) Subcellular localization of GFP-ERK3 is altered by the coexpression of Flag-tagged Sept7 in HeLa cells from uniform cytoplasmic localization to filamentous cytoplasmic structures. GFP transfected with Flag-Sept7 is shown as a control (scale bar, 5 μm). (C) FRET

the direct interaction of ERK3 and Sept7 in living cells, we then applied fluorescence resonance transfer (FRET) measurements using the expression of ECFP-Sept7 and EYFP-ERK3 in HeLa cells. The measured FRET efficiency, which was determined by the acceptor photobleaching technique (29) and which is shown in a false-color-coded manner (FRET eff in Fig. 3C), displays significant local values (red) and clearly demonstrates short-range interaction between ERK3 and Sept7.

Because of the possibility that ERK3 acts as a docking platform for both MK5 and Sept7 in parallel, we analyzed the localization of HA-MK5 and myc-Sept7 in the absence and presence of ERK3. When coexpressed with myc-Sept7 alone, HA-MK5 displays exclusive nuclear localization distinctly from the mainly cytoplasmic structures of myc-Sept7 (Fig. 3D). Interestingly, the coexpression of BE-ERK3 induces the colocalization of myc-Sept7 and HA-MK5 in filamentous cytoplasmic structures (Fig. 3D), indicating that MK5 and Sept7 can bind to ERK3 simultaneously and that this is the mechanism by which ERK3 targets MK5 to Sept7-containing filamentous cytoplasmic structures. To prove the direct interaction of all three proteins in a ternary complex, we performed the GST-MK5 pulldown of GFP-Sept7 in the absence and presence of His-ERK3. As a positive control, we applied the MK5 pulldown of GFP-tagged ERK3, which is efficiently enriched in the GST-MK5 pulldown fraction (Fig. 3E). However, GFP-Sept7 does not directly bind to GST-MK5 and is copurified in the pulldown only in the presence of ERK3. This experiment supports the notion that ERK3 acts as an adaptor or a docking platform for Sept7 and MK5.

ERK3 and MK5 reorganize endogenous Sept7. To demonstrate the role of ERK3/MK5 in the structural organization of septins, we analyzed endogenous Sept7 distribution in ERK3/MK5 double-deficient MEFs by immunocytochemistry. In these cells, Sept7 filament structure is weaker than that of double-deficient MEFs rescued with expression constructs of MK5 and ERK3 (Fig. 3F). Apparently, the rescue leads to a redistribution of endogenous Sept7 to more filamentous structures. Categorizing Sept7 filament structure into groups of weak, moderate, and strong filament formation for 100 cells in triplicate shows a significant shift to more filamentous structures in the presence of ERK3/MK5 (Fig. 3G). These results indicate a distinct role of the Sept7/ERK3/MK5 complex in the cellular context.

Identification of Kal7 as a novel interaction partner of MK5. To identify further proteins interacting with the ternary ERK3/MK5/Sept7 complex and decipher the neuronal signaling network, we applied a classical Y2H screen using MK5 as the bait and screened a mouse brain cDNA library (MY4008AH; Clontech). Interestingly, among other positive clones coding for ATPase subunit beta-1 (ATP1b1) and cell division cycle and apoptosis regulator protein 1 (Ccar1), we also identified the GDP exchange factor Kal7 and Septin 8 (Sept8) as proteins which specifically interact with MK5 but not with the related protein kinase MK2 (Fig. 4A and data not shown). Kal7 was previously shown to stimulate spine formation and maturation (36). It is a large multidomain protein of 1,663 amino acids. The MK5-interacting fragment (amino acids 588 to 946) isolated in the screen belongs to a region of nine distinct spectrin-like repeats (SR) (Fig. 4B). We verified interaction between MK5 and Kal7 by the copurification of endogenous MK5 in a GST pulldown from lysates of HEK293 cells with 10 μg recombinant GST fusion protein of Kal7 spectrin-like repeat SR4-7 (amino acids 517 to 976) and SR3-6 (amino acids 416 to 870), respectively. Both Kal7 fragments were able to bind endogenous MK5 in this pulldown (Fig. 4D), indicating that MK5 binds to the overlap containing SR4-6. To further demonstrate the *in vivo* relevance of the interaction between MK5 and Kal7, we expressed HA-tagged MK5 and myc-tagged Kal7 in HEK293 cells and analyzed their colocalization. MK5 and Kal7 show partial colocalization in the cytoplasmic compartment (Fig. 4C). In addition, the colocalization of both proteins in the cytoplasmic, perinuclear region is significantly increased when ERK3 is coexpressed together with the two proteins (data not shown).

Regulators of septin filaments and spine morphology can act as the substrates for the ERK3/MK5 complex. Using *in vitro* kinase assays with recombinant Sept7ΔN and Sept7ΔC, we could not detect any significant Sept7 phosphorylation by recombinant MK5 or ERK3 (see Fig. S2 in the supplemental material). Therefore, we asked whether other Sept7-interacting proteins which are involved in the regulation of filament structures could act as substrates of the ERK3/MK5 complex. A Sept6/7-specific regulator of filament assembly is Borg3, which, similarly to Borg1 and Borg2, binds to the septin GTPase domain (18, 43). We expressed recombinant GST-tagged Borg1 to Borg3 in *E. coli* and tested these proteins as substrates for ERK3 and MK5 in an *in vitro* kinase assay (Fig. 5A). Recombinant baculovirus-expressed 6×His-ERK3 possesses intrinsic activity and can efficiently phosphorylate Borg1, Borg2, and, to a lesser extent, Borg3 (Fig. 5A, middle). As a positive control for ERK3 catalytic activity, the pan-MAPK substrate MBP was employed (58). Using p38-activated GST-MK5 in the kinase assay, Borg2 could be phosphorylated *in vitro* with efficiency comparable to that of the known *in vitro* substrate Hsp25. Borg3 is also phosphorylated by MK5, albeit with lower efficiency (Fig. 5A, right).

We then tested whether Kal7 is phosphorylated by MK5. Interestingly, Kal7 was previously described as a substrate for caMKII, a protein kinase belonging to the same family as MK5 (56). *In vitro* phosphorylation assays revealed that a Kal7 fragment containing SR3-6, but not the fragment with SR4-7, is strongly phosphorylated in the presence of MK5 and its *in vitro* activator p38 MAPKα (Fig. 5C), indicating that the phosphorylation site for MK5 is lo-

measurements of the interaction of ECFP-Sept7 and EYFP-ERK3 in living HeLa cells by acceptor photobleaching. FRET efficiency (FRET Eff) is calculated from the donor fluorescence before (*D* pre) and after bleaching of the acceptor (*D* post) using the equation FRET Eff = 1 (*D* pre/*D* post), and results are shown by false color coding. The fluorescence of the donor and the acceptor (A) before and after bleaching are shown separately. (D) MK5 can bind to Sept7-bound ERK3 and relocalize to Sept7 filamentous structures (scale bar, 5 μm). (E) MK5 interaction with Sept7 is bridged by ERK3 binding. GST pulldown assay with GST-MK5 in HEK293 cells showed copurification of GFP-Sept7 only if ERK3 was also coexpressed. (F) Endogenous Sept7 filaments are less organized in ERK3/MK5 double-knockout MEFs. ERK3/MK5 knockout MEFs retrovirally rescued with ERK3 and MK5 (pMMP-MK5/pMMP-ERK3) showed a higher complexity of Sept7-containing filaments than the empty vector-transduced cells (pMMP). (G) Categorization of septin filament complexity performed for 100 of the differentially transduced cells in triplicate (standard deviations are indicated) into groups of weak, moderate, or strong filament organization. ERK3/MK5 retrovirally rescued cells showed a significantly higher number of moderate and strong septin filament-containing cells and a significantly lower number of cells displaying weak septin organization (one-tailed *t* test).

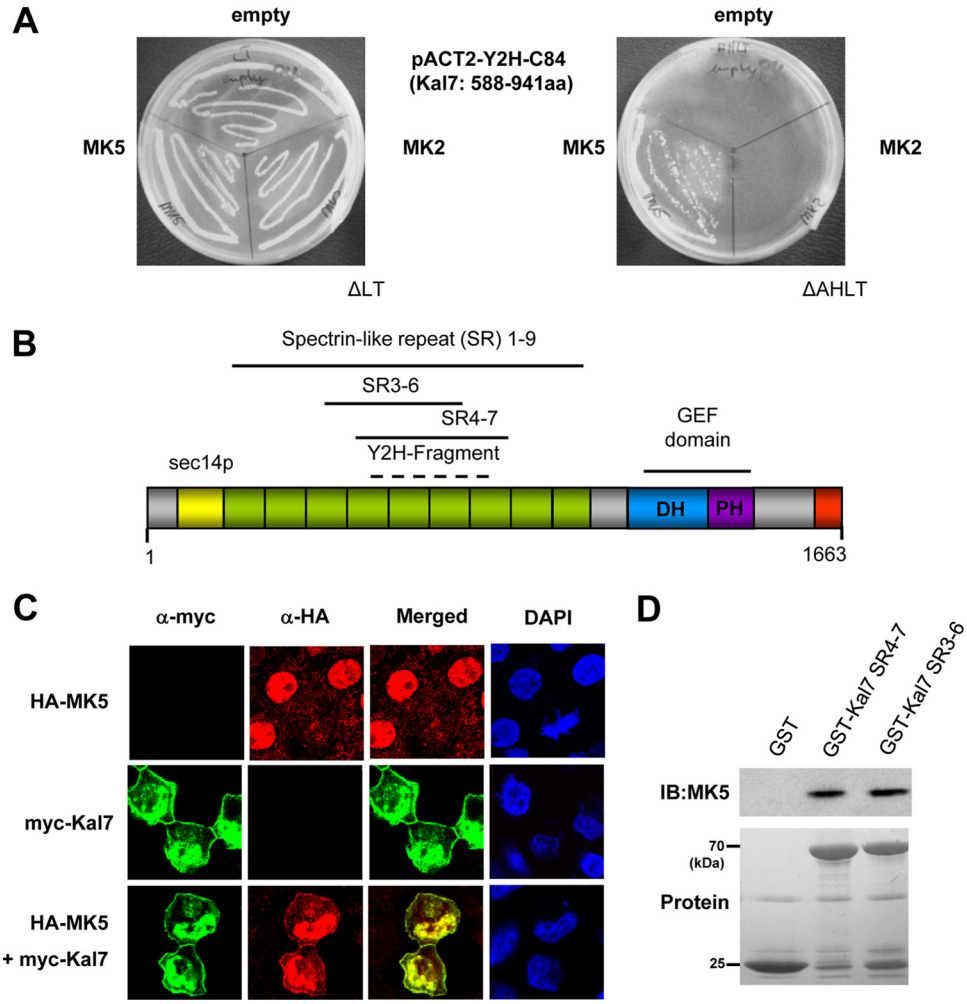

FIG 4 Identification and characterization of Kal7 as a novel MK5 interaction partner. (A) Identification of RhoGEF kalirin-7 (Kal7) as an MK5 interacting protein in a classical Y2H screen. pGBKT7-MK5 was used as bait for the screening of a brain cDNA library (Clontech). A cDNA clone expressing a 353-amino-acid fragment of Kal7 specifically interacts with MK5 but not with the related protein kinase MK2 or the empty bait vector. (B) Schematic representation of the domain structure and the MK5 interacting region of mouse Kal7 (DH, Dbl homology; GEF, guanosine nucleotide exchange factor; PH, pleckstrin homology; PDZ, PDZ binding motif [Ser-Thr-Tyr-Val]; sec14p, domain binding PIP2 [3, 5] and PIP3; and SR, spectrin-like repeat). (C) myc-Kal7 and HA-MK5 were coexpressed in HEK293 cells and analyzed by immunofluorescence. DAPI staining shows the nuclei in blue. (D) Pulldown of endogenous MK5 from HEK293 cells using GST-tagged fragments of Kal7 spanning spectrin-like repeats 3 to 6 or 4 to 7.

cated in SR3. SR3 contains an ideal consensus phosphorylation motif for MK5 (Fig. 5B) between amino acids 482 and 488. The mutation of S487 to alanine completely abolished the *in vitro* phosphorylation of SR3-6 by MK5 (SR3-6 S487A in Fig. 5C), demonstrating that S487 is the only phosphorylation site for MK5 in spectrin-like repeats 3 to 6. Incidentally, Kal7 S487 phosphorylation has already been detected by mass spectrometry in mouse brain extracts (14, 24). This phosphorylation site is located within an intramolecular PXXP ligand of the SH3 domain of kalirin and is proposed to stimulate guanosine nucleotide exchange factor (GEF) activity by preventing intramolecular SH3-PXXP interaction (40). This indicates a role for the ERK3/MK5 complex in Kal7 regulation.

Sept7-dependent enhancement of dendritic complexity and spine formation in *ex vivo*-cultured primary hippocampal neurons by ERK3/MK5. Sept7 was found in postsynaptic density fractions of the brain (35) and is localized at the base of dendritic protrusions and at dendritic branch points in cultured hippocampal neurons (51, 55). Interestingly, the overexpression of Sept7 increased dendrite branching to a certain degree, and more importantly, the knockdown of Sept7 led to a greater proportion of immature dendritic protrusions and impaired dendritic branching (51, 55). To directly analyze the effect of the ERK3/MK5/Sept7 module in neuronal morphogenesis, we decided to perform dual-overexpression studies in mouse hippocampal neurons. Neurons were isolated from embryonic day 18 BALB/c mice (E18.5) and cultivated on coated glass coverslips. After 5 days of *in vitro* culture cells were transfected with pcDNA6/BioEase-ERK3, pcDNA3.1-HA-MK5, or pRK5-myc-Sept7 together with pEGFP to enable the visualization of transfected neurons. For the initial analysis of neuronal morphology, transfected cells were analyzed 3 days later (5 + 3DIV) for dendrite number and branching. The overall complexity of statistically relevant, selected neurons transfected with pEGFP alone (CTRL) or with pRK5-myc-Sept7/pEGFP only

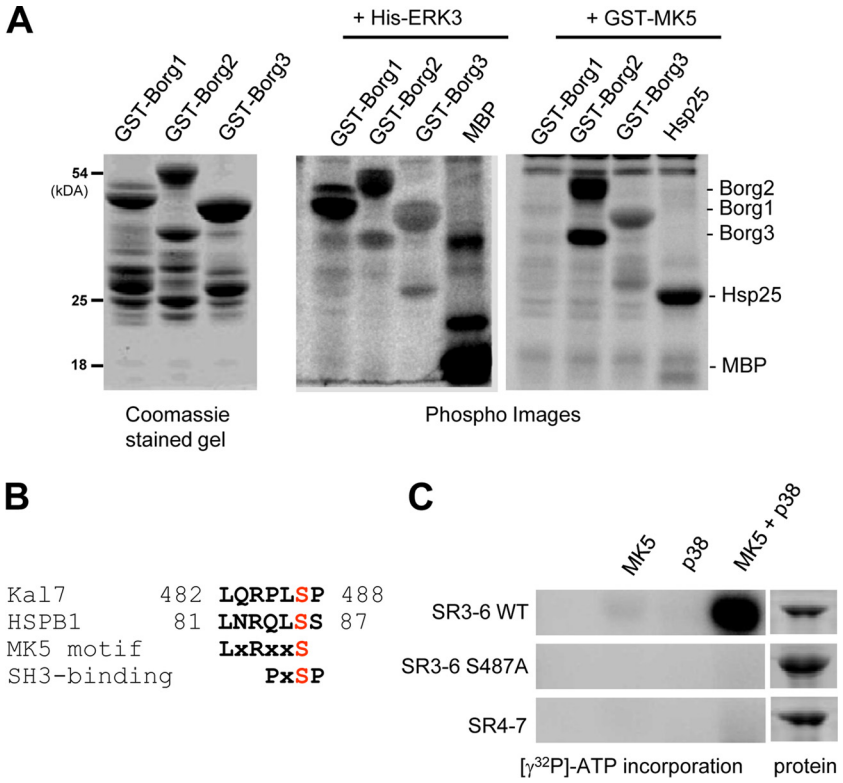

FIG 5 Borg1 to Borg3 and Kal7 as *in vitro* substrates of ERK3 and MK5. (A) *In vitro* phosphorylation of Borg1, Borg2, and Borg3 by ERK3 and MK5. Recombinant GST-tagged Borg1, Borg2, and Borg3 were expressed in *E. coli* and used for *in vitro* kinase assays with Sf9-expressed, active His-ERK3 or with *E. coli*-expressed, p38-activated GST-MK5. Incorporated phosphate from [γ-^{33}P]ATP was detected by phosphorimaging. As positive controls, the known ERK3 substrate myelin basic protein (MBP) and the known MK5 substrate heat shock protein beta-1 (Hspb1; Hsp25) were used. ERK3 phosphorylates all Borg proteins, especially Borg1 and Borg2, whereas MK5 preferentially phosphorylates Borg2. This correlates with the existence of phosphorylation site consensus motifs identified in these proteins. (B) Alignment of MK5 consensus phosphorylation motif in Kal7 to that in the *in vitro* substrate Hspb1. Kal7-S 487 is located in an ideal MK5 consensus motif, LXRXXS*, and a putative SH3-binding PXS*P motif. (C) Identification of the MK5 phosphorylation site in Kal7. The fragment SR3-6, but not the mutated fragment SR3-6-S487A, is phosphorylated by MK5. Phosphorylation was detected by ^{32}P incorporation and phosphorimaging.

(Sept7) or together with pcDNA6/BioEase-ERK3 and pcDNA3.1-HA-MK5 (ERK3/MK5/Sept7) was analyzed by fluorescence microscopy and is shown in Fig. 6A. While septin7 alone does not significantly increase neuronal complexity, the coexpression of ERK3/MK5 leads to obviously more complex neurons possessing more dendrites with apparently more branches. Sholl analysis counts the number of intersections made by dendrites with concentric circles of increasing distance from the cell body, reflecting both dendrite numbers and intersections and thus representing a very sensitive and objective measure (47). We employed this analysis on a statistically relevant number of each set of differentially transfected neurons. The expression of Sept7, MK5, ERK3, or ERK3/MK5 together only with the enhanced GFP (EGFP) construct does not lead to an increase in the Sholl index (Fig. 6B). However, MK5 and ERK3 lead to a highly significant increase in Sholl intersections of the transfected neurons at all distances from the soma when coexpressed with Sept7 ($n = 16$). These data clearly indicate a ERK3/MK5-dependent septin7 function in the regulation of neuronal morphogenesis.

Since septin7 has also been described to alter dendritic spine morphology (55) and MK5 deficiency was associated with reduced spine numbers *in vivo*, we analyzed spine numbers in the differently transfected neurons in detail. The number of spines displays a significant increase only in ERK3/MK5/Sept7-expressing dendrites (Fig. 6C). We extended the analysis to cover later stages of neuronal differentiation by transfecting primary neurons at DIV10 and inspecting morphology at DIV15 (Fig. 6D). In cells expressing only Sept7, dendritic complexity and spine formation is rather low and does not significantly differ from that of control cells (not shown). Again, the expression of Sept7 together with ERK3 and MK5 (ERK3/MK5/Sept7) leads to dramatically increased dendritic complexity. In addition, spine formation is significantly increased in number and size in these cells (Fig. 6D, insets). These results support the notion that the ERK3/MK5 complex modulates dendritic complexity and spine formation via septin-dependent processes.

DISCUSSION

We observed the impaired spine formation of hippocampal neurons *in vivo* in mice lacking MK5 and also displaying reduced levels of ERK3 (41, 44). This could explain the complex behavioral phenotypes associated with ERK3 deficiency and caMK5 transgenic mouse models. In search of neurologically relevant players associated with the ERK3/MK5 signaling module, we identified Sept7 and Kal7 as novel interacting partners of ERK3 and MK5, respectively. Sept7 is a characteristic member of the GTP-binding septin family that is involved in various structural remodelling processes of the eukaryotic cells, ranging from the budding of

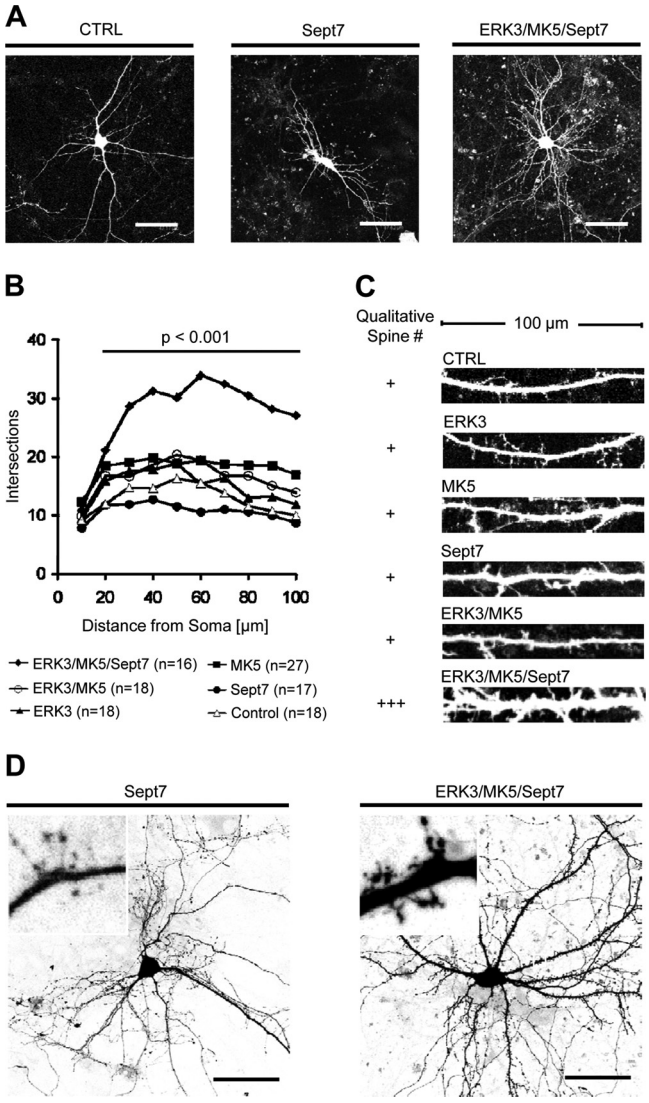

FIG 6 Sept7-dependent stimulation of dendritic outgrowth and increased spine number by overexpression of the ERK3/MK5 complex in primary hippocampal neurons. Primary neurons were isolated at embryonic day 18. Transfection was carried out with BE-tagged ERK3, HA-tagged MK5, myc-tagged Sept7, or their combinations together with pEGFP at DIV5 (A to C) or DIV10 (D). Seventy-two (A to C) or 120 (D) h posttransfection, cells were fixed and analyzed using confocal microscopy. (A) Representative images of statistically relevant neurons overexpressing GFP (CTRL), Sept7, or a combination of ERK3, MK5, and Sept7 (scale bar, 50 μm). (B) Sholl analysis of neurons differently transfected with the constructs coding for the indicated proteins and EGFP. (C) Qualitative analysis of dendritic spine morphology from the experiment shown in panel B. (D) Representative images of primary neurons expressing EGFP and Sept7 or ERK3/MK5/Sept7, respectively (scale bar, 50 μm). Insets display spine morphology.

yeast to cilium and dendritic spine formation in mammalian cells (4). Kal7 is a GDP exchange factor regulated by phosphorylation, and it contributes to the functional plasticity of neurons (36, 56). While Kal7 is directly phosphorylated by MK5 *in vitro*, Sept7 does not act as a direct ERK3 or MK5 substrate. However, the physical interaction of the ERK3/MK5 module with Sept7 could bring this complex closer to septin filaments and potential other substrates interacting with these filaments. Accordingly, we could demonstrate that the septin-interacting and -regulating Borg proteins (Borg1 to Borg3) are direct substrates for ERK3 and MK5 *in vitro*. Viewed together, these results strongly suggest a complex role of the ERK3/MK5 signaling module in the regulation of neuronal cytoskeleton and dendritic spine formation. We also identified Sept8 as an interaction partner for MK5. Recently, it has been shown that Sept7 can form dimers and trimers consisting of Sept7/Sept8, Sept2/Sept8/Sept7, and Sept5/Sept8/Sept7 (39). This raises the possibility that ERK3, which binds Sept7, and MK5, which binds Sept8, cooperate in their binding to specific heterodimeric and trimeric Sept7/8-containing complexes.

Using transfected primary neurons, we demonstrated a Sept7-dependent function of the ERK3/MK5 module in neuronal morphology, dendrite outgrowth, and spine formation. This finding is in agreement with the prominent role of Sept7 in neuronal morphogenesis (51, 55) and adds a new level of regulation by the ERK3/MK5 module. The effects of ERK3/MK5/Sept7 on neuronal morphogenesis observed are complex and quantified by dendrite number, number of branches, and spine density. However, we also have the impression that the dendritic shafts are significantly thicker, and that many of the spines are rather compact and also could result from incomplete branching. This could be due to overexpression effects, which disturb the homeostasis of morphogenesis, or could represent other unknown functions of septins in neurons. So far, we are not able to demonstrate a direct involvement of the phosphorylation of Kal7 or Borg1 to Borg3 by ERK3/MK5 in the Sept7-dependent effects. This requires further detailed analysis using phosphorylation mutants of these proteins or the combination of overexpression of ERK3/MK5/Sept7 with the knockdown of Kal7 and/or Borg proteins in primary neurons.

The function of the ERK3/MK5-Sept7 signaling module in spine morphogenesis could explain the diminished spine numbers in the MK5-deficient mice. Thus, the *in vitro* transfection studies perfectly complement the *in vivo* phenotype. Sept7 staining in the neurons from MK5 knockout animals did not show significant differences (data not shown). However, it could well be that the impairment in the formation of novel septin filaments leads to decreased numbers of spines with similar steady-state morphology and septin content. There could be other players involved or changes in the septin interactome induced by ERK3/MK5 signaling. Although the data presented here clearly demonstrate that Sept7 needs to be present to produce the ERK3/MK5-dependent morphological effects, we cannot exclude that Borg1 to Borg3, Kal7, or further unknown substrates are also involved. To this end, it is interesting that in mouse brain the extensive phosphorylation of Kal7 in the spectrin-like repeat region, including the MK5 site S487 identified here, has been demonstrated recently (24). Furthermore, kalirin knockout mice display decreased hippocampal spine density (30), and the overexpression of Kal7 induces spine enlargement (56), supporting the notion of a contribution of Kal7 in spine formation (Fig. 7).

The impaired generation of neuronal structures and reduced neuronal plasticity may have dramatic consequences in embryonic development, and it could explain the poorly understood perinatal and embryonic lethality displayed by ERK3 and MK5 knockout mice, respectively (25, 41). For ERK3 knockout mice, the perinatal lethality is due to acute respiratory failure within minutes of birth, although these animals display normal lung-branching morphogenesis. Also, the *in utero* administration of glucocorticoid promoted fetal lung maturity but failed to rescue

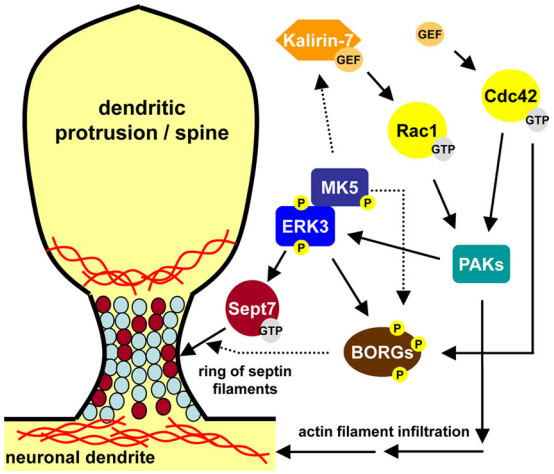

FIG 7 Neuronal ERK3/MK5/Sept7 signaling and spine morphogenesis. The ERK3/MK5/Sept7 signaling complex is activated by Cdc42 and Rac GTPase via p21-activated protein kinases (PAKs). Septin heteromeric structures are generated via the ERK3/MK5/Sept7-mediated recruitment and phosphorylation of Borg proteins. The MK5 substrate Kal7, a Rho GEF and known activator of Rac GTPases, further contributes to PAK activation and actin filament reorganization. Thus, the coordinated phosphorylation of Borg proteins and Kal7 by ERK3 and MK5 constitute a novel signaling cascade involving feed-forward circuits, multiple GTPases, and cytoskeletal elements.

the lethal phenotype of this mouse strain (25). One can speculate that respiratory rhythm-generating neurons residing within the hindbrain are impaired in their functional cooperativity by the reduced ability to form dendrites and spines. A similar scenario in other specific brain regions could explain the enigmatic embryonic lethality with incomplete penetrance seen in MK5-deficient mice when backcrossed to the C57BL/6J strain, which does not correlate with any morphological and histological abnormalities in peripheral tissues (41). Furthermore, lower neuronal complexity in the hippocampus, as detected for spines in MK5-deficient mice, could cause deficiency in long-term memory and, especially, disoriented behavior and impaired place navigation (32), as occasionally observed by us with this strain (A. Kotlyarov and T. Yakovleva, unpublished data).

Besides the ERK3/MK5 complex, a similar functional interaction has been demonstrated between ERK4 and MK5 (1, 19). Although the C-terminal extension of ERK4 (amino acids 312 to 583) is significantly shorter than the C terminus of ERK3 (amino acids 316 to 720) and displays sequence similarities to ERK3 only in the region between amino acids 312 and 462, the first pulldown experiments demonstrated an interaction between ERK4 and Sept7 (S. Kant, unpublished data). This indicates that the septin interaction domain of ERK3 is located between 358 and 481 (the residue homologous to amino acid 462 in ERK4). Extending the functional Sept7 experiments to ERK4 is interesting, since ERK4 is also highly expressed in brain, and its deficiency is associated with depression-related behavior in mice (38). A common MK5/septin-dependent neuronal signaling module associated with the differential expression of the kinases in neuronal cells could explain nonredundant neuronal function and the difference between the phenotypes of the ERK3 and ERK4 knockout mice (38).

Phosphorylation by caMKII and the translocation of the brain-specific neuronal guanine nucleotide exchange factor and novel MK5 interactor Kal7 from dendrite shafts into nearby spines leads to the activation of the Rac1 target PAK in spines (28). Interestingly, members of the PAK family of protein kinases have recently been identified as activators for ERK3 and ERK4, which phosphorylate serines 189 and 186 within the atypical activation loop motif SEG of ERK3 and ERK4, respectively. Hence, the Kal7-mediated PAK-dependent activation of the ERK3/MK5 module could further stimulate the Sept7-dependent remodelling of septin filaments. The subsequent phosphorylation of Kal7 by MK5 could represent a feed-forward control of this activation process by the stimulation of its GEF activity for Rac1 (Fig. 7).

While various functions of the p38/MK5 (p38/PRAK) module have been described, ranging from oncogenesis and senescence (50) to metabolic restriction (57), the physiological function of the well-characterized ERK3/MK5 complex was enigmatic until recently. By analyzing the neuronal morphology in MK5-deficient mice and complementing it with large-scale screening methodologies and *in vitro* neuronal culture manipulations, we describe a novel role for the ERK3/MK5 signaling module in the Sept7-dependent regulation of neuronal morphogenesis. This function might explain the pleiotropic behavioral and developmental phenotypes of the ERK3 and MK5 knockout mice and could be of relevance to other septin-dependent processes in mammalian cells.

ACKNOWLEDGMENTS

We thank Ami Aronheim (The Rappaport Institute, Israel), Ole-Morten Seternes (University of Tromso, Norway), Koh-ichi Nagata (Aichi Human Service Center, Japan), Betty Eipper (University of Connecticut), and Ian Macara (University of Virginia School of Medicine) for providing plasmid constructs and Ole-Morten Seternes (University of Tromso, Norway), Anne Hennig (Hannover Medical School), and ProQinase Gmbh (University of Freiburg) for recombinant proteins. We thank Evgeni Ponimaskin and Daria Guseva for technical support in setting up primary neuronal cultures, Rudolf Bauerfeind for technical support for the FRET measurements, and Juri Lafera (Hannover Medical School) for help with the cloning of recombinant plasmids.

This work was supported by Deutsche Forschungsgemeinschaft KO2091/1 (to A.K. and M.G.) and by a grant from the Canadian Institutes of Health Research (to S.M.).

REFERENCES

1. **Aberg E, et al.** 2006. Regulation of MAPK-activated protein kinase 5 activity and subcellular localization by the atypical MAPK ERK4/MAPK4. J. Biol. Chem. **281**:35499–35510.
2. **Aberg E, et al.** 2009. Docking of PRAK/MK5 to the atypical MAPKs ERK3 and ERK4 defines a novel MAPK interaction motif. J. Biol. Chem. **284**: 19392–19401.
3. **Barral Y.** 2010. Cell biology. Septins at the nexus. Science **329**:1289–1290.
4. **Barral Y, Mansuy IM.** 2007. Septins: cellular and functional barriers of neuronal activity. Curr. Biol. **17**:R961–R963.
5. **Broder YC, Katz S, Aronheim A.** 1998. The ras recruitment system, a novel approach to the study of protein-protein interactions. Curr. Biol. **8**:1121–1124.
6. **Cheng M, et al.** 1996. Characterization of a protein kinase that phosphorylates serine 189 of the mitogen-activated protein kinase homolog ERK3. J. Biol. Chem. **271**:12057–12062.
7. **Coulombe P, Meloche S.** 2007. Atypical mitogen-activated protein kinases: structure, regulation and functions. Biochim. Biophys. Acta **1773**: 1376–1387.
8. **De la Mota-Peynado A, Chernoff J, Beeser A.** 2011. Identification of the atypical MAPK Erk3 as a novel substrate for p21-activated kinase (Pak) activity. J. Biol. Chem. **286**:13603–13611.
9. **Deleris P, et al.** 2008. Activation loop phosphorylation of the atypical MAP kinases ERK3 and ERK4 is required for binding, activation and cytoplasmic relocalization of MK5. J. Cell. Physiol. **217**:778–788.

10. **Deleris P, et al.** 2011. Activation loop phosphorylation of ERK3/ERK4 by group I p21-activated kinases (PAKs) defines a novel PAK-ERK3/4-MAPK-activated protein kinase 5 signaling pathway. J. Biol. Chem. **286**: 6470–6478.
11. **Dobbelaere J, Gentry MS, Hallberg RL, Barral Y.** 2003. Phosphorylation-dependent regulation of septin dynamics during the cell cycle. Dev. Cell **4**:345–357.
12. **Feng G, et al.** 2000. Imaging neuronal subsets in transgenic mice expressing multiple spectral variants of GFP. Neuron **28**:41–51.
13. **Gerits N, Van Belle W, Moens U.** 2007. Transgenic mice expressing constitutive active MAPKAPK5 display gender-dependent differences in exploration and activity. Behav. Brain Funct. **3**:58.
14. **Gnad F, Gunawardena J, Mann M.** 2011. PHOSIDA 2011: the posttranslational modification database. Nucleic Acids Res. **39**:D253–D260. doi: 10.1093/nar/gkq1159.
15. **Gonzalez FA, Raden DL, Rigby MR, Davis RJ.** 1992. Heterogeneous expression of four MAP kinase isoforms in human tissues. FEBS Lett. **304**:170–178.
16. **Hansen CA, Bartek J, Jensen S.** 2008. A functional link between the human cell cycle-regulatory phosphatase Cdc14A and the atypical mitogen-activated kinase Erk3. Cell Cycle **7**:325–334.
17. **Heimrich B, Frotscher M.** 1991. Differentiation of dentate granule cells in slice cultures of rat hippocampus: a Golgi/electron microscopic study. Brain Res. **538**:263–268.
18. **Joberty G, et al.** 2001. Borg proteins control septin organization and are negatively regulated by Cdc42. Nat. Cell Biol. **3**:861–866.
19. **Kant S, et al.** 2006. Characterization of the atypical MAPK ERK4 and its activation of the MAPK-activated protein kinase MK5. J. Biol. Chem. **281**:35511–35519.
20. **Kim SK, et al.** 2010. Planar cell polarity acts through septins to control collective cell movement and ciliogenesis. Science **329**:1337–1340.
21. **Kinoshita M.** 2003. Assembly of mammalian septins. J. Biochem. **134**: 491–496.
22. **Kinoshita M.** 2006. Diversity of septin scaffolds. Curr. Opin. Cell Biol. **18**:54–60.
23. **Kinoshita, M.** 2003. The septins. Genome Biol. **4**:236.
24. **Kiraly DD, et al.** 2011. Identification of kalirin-7 as a potential postsynaptic density signaling hub. J. Proteome Res. **10**:2828–2841.
25. **Klinger S, et al.** 2009. Loss of Erk3 function in mice leads to intrauterine growth restriction, pulmonary immaturity, and neonatal lethality. Proc. Natl. Acad. Sci. U. S. A. **106**:16710–16715.
26. **Kress TR, et al.** 2011. The MK5/PRAK kinase and Myc form a negative feedback loop that is disrupted during colorectal tumorigenesis. Mol. Cell **41**:445–457.
27. **Lein ES, et al.** 2007. Genome-wide atlas of gene expression in the adult mouse brain. Nature **445**:168–176.
28. **Liao D, Scannevin RH, Huganir R.** 2001. Activation of silent synapses by rapid activity-dependent synaptic recruitment of AMPA receptors. J. Neurosci. **21**:6008–6017.
29. **Lippincott-Schwartz J, Snapp E, Kenworthy A.** 2001. Studying protein dynamics in living cells. Nat. Rev. Mol. Cell Biol. **2**:444–456.
30. **Ma XM, et al.** 2008. Kalirin-7 is required for synaptic structure and function. J. Neurosci. **28**:12368–12382.
31. **Martinez C, et al.** 2004. Mammalian septin function in hemostasis and beyond. Exp. Biol. Med. **229**:1111–1119.
32. **Morris RG, Garrud P, Rawlins JN, O'Keefe J.** 1982. Place navigation impaired in rats with hippocampal lesions. Nature **297**:681–683.
33. **Mostowy S, Cossart P.** 2012. Septins: the fourth component of the cytoskeleton. Nat. Rev. Mol. Cell Biol. **13**:183–194.
34. **New L, Jiang Y, Han J.** 2003. Regulation of PRAK subcellular location by p38 MAP kinases. Mol. Biol. Cell **14**:2603–2616.
35. **Peng J, et al.** 2004. Semiquantitative proteomic analysis of rat forebrain postsynaptic density fractions by mass spectrometry. J. Biol. Chem. **279**: 21003–21011.
36. **Penzes P, et al.** 2003. Rapid induction of dendritic spine morphogenesis by trans-synaptic ephrinB-EphB receptor activation of the Rho-GEF kalirin. Neuron **37**:263–274.
37. **Perander M, et al.** 2008. The serine 186 phospho-acceptor site within ERK4 is essential for its ability to interact with and activate PRAK/MK5. Biochem. J. **411**:613–622.
38. **Rousseau J, et al.** 2010. Targeted inactivation of Mapk4 in mice reveals specific nonredundant functions of Erk3/Erk4 subfamily mitogen-activated protein kinases. Mol. Cell. Biol. **30**:5752–5763.
39. **Sandrock K, et al.** 2011. Characterization of human septin interactions. Biol. Chem. **392**:751–761.
40. **Schiller MR, et al.** 2006. Regulation of RhoGEF activity by intramolecular and intermolecular SH3 domain interactions. J. Biol. Chem. **281**:18774–18786.
41. **Schumacher S, et al.** 2004. Scaffolding by ERK3 regulates MK5 in development. EMBO J. **23**:4770–4779.
42. **Seternes OM, et al.** 2004. Activation of MK5/PRAK by the atypical MAP kinase ERK3 defines a novel signal transduction pathway. EMBO J. **23**: 4780–4791.
43. **Sheffield PJ, et al.** 2003. Borg/septin interactions and the assembly of mammalian septin heterodimers, trimers, and filaments. J. Biol. Chem. **278**:3483–3488.
44. **Shi Y, et al.** 2003. Elimination of protein kinase MK5/PRAK activity by targeted homologous recombination. Mol. Cell. Biol. **23**:7732–7741.
45. **Shiryaev A, Dumitriu G, Moens U.** 2011. Distinct roles of MK2 and MK5 in cAMP/PKA- and stress/p38MAPK-induced heat shock protein 27 phosphorylation. J. Mol. Signal. **6**:4.
46. **Shiryaev A, Moens U.** 2010. Mitogen-activated protein kinase p38 and MK2, MK3 and MK5: menage a trois or menage a quatre? Cell. Signal. **22**:1185–1192.
47. **Sholl DA.** 1953. Dendritic organization in the neurons of the visual and motor cortices of the cat. J. Anat. **87**:387–406.

47a. **Sirajuddin M, et al.** 2007. Structural insight into filament formation by mammalian septins. Nature **449**:311–315.

48. **Spiliotis ET, Kinoshita M, Nelson WJ.** 2005. A mitotic septin scaffold required for mammalian chromosome congression and segregation. Science **307**:1781–1785.
49. **Spiliotis ET, Nelson WJ.** 2006. Here come the septins: novel polymers that coordinate intracellular functions and organization. J. Cell Sci. **119**: 4–10.
50. **Sun P, et al.** 2007. PRAK is essential for ras-induced senescence and tumor suppression. Cell **128**:295–308.
51. **Tada T, et al.** 2007. Role of septin cytoskeleton in spine morphogenesis and dendrite development in neurons. Curr. Biol. **17**:1752–1758.
52. **Turgeon B, Meloche S.** 2009. Interpreting neonatal lethal phenotypes in mouse mutants: insights into gene function and human diseases. Physiol. Rev. **89**:1–26.
53. **Unger T, Jacobovitch Y, Dantes A, Bernheim R, Peleg Y.** 2010. Applications of the restriction free (RF) cloning procedure for molecular manipulations and protein expression. J. Struct. Biol. **172**:34–44.
54. **Vrabioiu AM, Mitchison TJ.** 2006. Structural insights into yeast septin organization from polarized fluorescence microscopy. Nature **443**:466–469.
55. **Xie Y, et al.** 2007. The GTP-binding protein Septin 7 is critical for dendrite branching and dendritic-spine morphology. Curr. Biol. **17**:1746–1751.
56. **Xie Z, et al.** 2007. Kalirin-7 controls activity-dependent structural and functional plasticity of dendritic spines. Neuron **56**:640–656.
57. **Zheng M, et al.** 2011. Inactivation of Rheb by PRAK-mediated phosphorylation is essential for energy-depletion-induced suppression of mTORC1. Nat. Cell Biol. **13**:263–272.
58. **Zhu AX, Zhao Y, Moller DE, Flier JS.** 1994. Cloning and characterization of p97MAPK, a novel human homolog of rat ERK-3. Mol. Cell. Biol. **14**:8202–8211.